Reduced Scale Model for Fixed Offshore Structures

by N. Roitman, R.C. Batista and F.L.L.B. Carneiro

ABSTRACT—A hydroelastic reduced scale model of a jacket-type offshore structure was designed and constructed according to the principles of physical similitude. The techniques employed for physical modeling, construction and experimental analysis are outlined briefly and some results from free and forced vibration tests are reported. Along with these test results, some comments are made on the damping-factor components obtained, effects of mass variation and changes on the vibration responses due to the loss of structural integrity.

Introduction

It is common practice in the design of offshore structures to use certain factors as prescribed by existing design rules. As these rules are often based on insufficient information, there is a need for more investigation. These factors are generally based on measured data obtained from a rather small number of prototypes. The limited experimental observation of these prototype structures is not sufficient to understand their dynamic behavior and consequently to determine relevant parameters for design. Observation has been limited due to difficulties found in isolating such various factors as geometric characteristics, structural shapes, type of foundations, soil, water depths, sea states in distinct measurement campaigns, wind, and variation of mass on the deck.

On the other hand, reduced-scale-model experiments are less expensive and have the advantage of allowing the isolation of the dominant factors which affect the dynamic behavior of these structures. Damping is one of the most important factors. Its distinct components can be determined best through careful laboratory experiments.

A paper by Carneiro,[1] which gives the similitude conditions for offshore type of structures, serves as a basis for the theoretical development of the present work.[2-6]

The techniques used in the design and construction of a reduced scale hydroelastic model of a fixed offshore structure are emphasized. How to use the experimental results to adjust the theoretical-numerical model developed to interpret the data acquired by structural monitoring is shown.

The Similitude Theory

Using the Vaschy-Buckingham theorem, seven independent dimensionless parameters were determined.[1] These parameters express the following similitude conditions:

$$\Pi_1 = \frac{T_s}{L_s}\left(\frac{E_s}{\varrho_s}\right)^{1/2} \tag{1}$$

$$\Pi_2 = \frac{\varrho_f}{\varrho_s} \tag{2}$$

$$\Pi_3 = \frac{H_f \cdot L_s}{T_f \cdot \nu_f} \tag{3}$$

$$\Pi_4 = \frac{H_f}{L_s} \tag{4}$$

$$\Pi_5 = T_f \cdot \left(\frac{g}{H_f}\right)^{1/2} \tag{5}$$

$$\Pi_6 = \frac{F}{\varrho_f \cdot g = L_s^3} \tag{6}$$

$$\Pi_7 = \xi_s + \xi_f \tag{7}$$

where, for an offshore structure,

L_s = a characteristic geometric dimension of the structure
H_f = the wave height
E_s = the elastic modulus
ϱ_s, ϱ_f = the structural material and fluid densities
T_f = the wave period
ν_f = the kinematic viscosity of the fluid
g = the gravity acceleration
ξ_s, ξ_f = the structural and fluid damping factors
F = force (e.g., wave forces, elastic forces)

The subscripts s and f relate to the structure and fluid, respectively.

To comply with the theoretical conditions of hydroelastic structural similitude, it is necessary to satisfy all the 'Π numbers' simultaneously. To do so requires that: (a) the material which constitutes the model has a low value of elastic modulus and a high density; (b) the fluid in which the model is immersed has a higher density than water and a kinematic viscosity approximately the same as water; (c) the damping factors, hysteretic for the model in air and hydrodynamic due to interaction with the fluid, have approximately the same value for the model as for the prototype.

Some of the scales used in the model are

$$k_F = k_L^3 \tag{8}$$

$$k_T = (k_L)^{1/2} \tag{9}$$

$$k_f = 1/(k_L)^{1/2} \tag{10}$$

$$k_{ac} = 1 \tag{11}$$

$$k_\sigma = k_L \tag{12}$$

$$k_m = k_L^3 \tag{13}$$

N. Roitman is Adjoint Professor, and R.C. Batista and F.L.L.B. Carneiro are Titular Professors, COPPE/UFRJ, Civil Engineering Program, Postal 68506 - R.J. Brazil.

Original manuscript submitted: September 1, 1986. Final manuscript received: March 31, 1989.

where

k_L = the geometric scale
k_F = the force scale
k_T = the period of time scale
k_f = the frequency scale
k_{ac} = the acceleration scale
k_σ = the normal tension scale
k_m = the mass scale

Model Design and Construction

The model constructed for observation of the physical behavior in air and in the fluid is of a $\frac{1}{70}$ geometric scale. The prototype belongs to a family of modulated four-legged tower type of fixed platform for water depths as great as 100 meters. These structures have currently been used in water depths around 70 meters along the Brazilian coast.

Figures 1(a) and 1(b) show a front view and two typical sections of the model. They give an idea of the model's general dimensions. In this figure the tubular members are numbered from (1) to (10) according to their cross sections which are given in Table 1. In this table the ideal model is the one that theoretically obeys all the similitude conditions; while the actual model simultaneously satisfies the seven 'Π numbers' [eqs (1)–(7)] using a distorted scale for the wall thickness of the tubular members with circular cross sections. It should be mentioned that piles numbered as members (1) in this table have been suppressed in the actual model, where members (2) take the mass and stiffness properties of both ideal members (1) plus (2) as a whole. The two cross sections shown in Fig. 1(b) are located in alternate levels along the model height.

To comply with one of the conditions (item a) imposed by the similitude theory, the model was constructed of plastic tubes (ABS polymer, which has a low elastic modulus compared to steels) filled with Mercury to reach the required model material density. This is shown in Fig. 1(c), where it can be seen that Mercury fills up the inner tube and is used in alternate longitudinal portions of the outer tube. This was achieved by gluing to the inner tube pieces of rubber with the shapes in cross section AA, and then inserting the inner tube into the main outer tube. To avoid air inside the tubes and fluid sloshing effects, the Mercury was carefully injected with a syringe through a silicone cap placed at tube ends. Simple flexion tests showed that the bending stiffness of a tubular member did not change by the addition of the inner tubing plus rubber pieces used.

The design, construction and assessment of the first natural frequencies of the model were carried out in parallel with the adjustment of the involved parameters (material density and members stiffness, deck mass and global stiffness, water added mass to stiffness ratio) through an integrated theoretical-numerical-experimental analysis.[2]

To match the moment of inertia of the mass at the top of the structure, eccentric lumps of lead were attached at

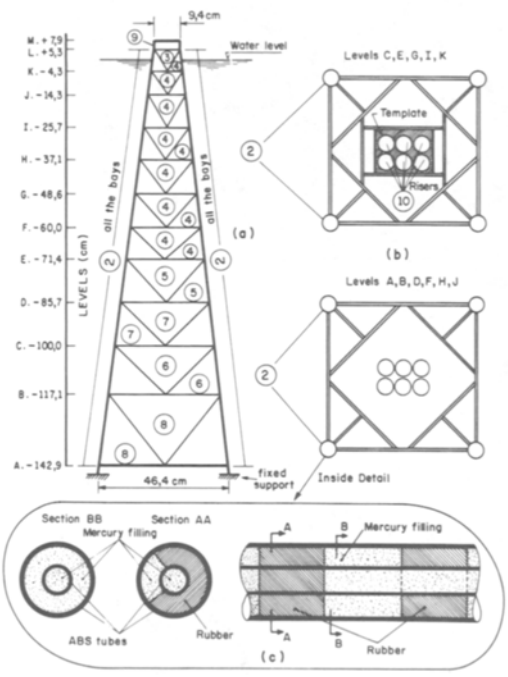

Fig. 1—Front view and typical model cross sections

TABLE 1—GEOMETRIC CHARACTERISTICS OF TUBULAR MEMBERS

	Prototype	Ideal Model	Actual Model
	$D \times d$ (cm)	$D \times d$ (mm)	$D \times d$ (mm)
(1) (piles)	76.20 × 4.45	10.89 × 0.66	suppressed
(2) (legs)	86.40 × 2.54	12.34 × 0.38	12.60 × 1.60
(3)	40.60 × 2.54	5.80 × 0.38	6.30 × 1.55
(4)	32.40 × 1.90	4.63 × 0.28	4.80 × 1.20
(5)	40.60 × 1.90	5.80 × 0.28	6.30 × 1.55
(6)	59.80 × 1.90	7.26 × 0.28	7.90 × 1.70
(7)	45.70 × 1.90	6.53 × 0.28	6.30 × 1.55
(8)	61.00 × 1.90	8.71 × 0.28	9.40 × 1.55
(9) (deck)	200.66 × 25.40	28.66 × 3.70	32.00 × 2.10
(10) (risers)	76.20 × 2.54	10.89 × 0.38	11.10 × 1.75

D = external diameter; d = wall thickness
ABS elastic modulus = 3252.5 N/mm²

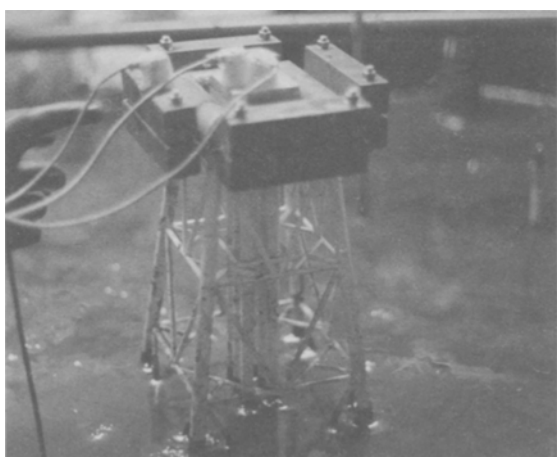

Fig. 2—The reduced model immersed in the modeling fluid

the deck level, thus adjusting torsional natural frequencies. These lumps of eccentric masses which can be seen in Fig. 2 are also illustrated in Fig. 3(a). Moreover, to compensate for the higher axial stiffness of the actual model legs, as compared to the ideal model (see Table 1), an additional lump of lead was attached to the center of the model top. The aim was to recover the axial strain along the legs by increasing the axial force on the structural components. All these lumps of masses located on the top of the model allowed the adjustment of both torsional plus flexural frequencies and modes.

The theoretical-numerical modeling was done with the use of the finite-element technique taking into account the results obtained from the similitude theory. The supports were taken as rigid and the deck had equivalent values for mass and stiffness taken from the experimental model.

The numerical modeling of the prototype and of the idealized reduced model (that is, the one to be fabricated) was realized seeking an adjustment based mainly on the correlation of the frequency responses, i.e., in a manner which brought close together the results for the natural frequencies obtained from the idealized model and from the similitude theory.

$$f_{model} = (1/\sqrt{k_L})\, f_{prot}$$

Experimental Procedure

Free and forced vibration tests were carried out on the model in air and immersed in water and heavy fluids (see Fig. 2), the latter having average densities of 1.45 g/cm³, 1.61 g/cm³ and 2.5 g/cm³. These fluid densities were achieved by mixing together water and powder of iron ore, closely approximating the ideal fluid density—2.7 g/cm³—given by the similitude theory. As each test could be performed in about 15 minutes, all the dynamic signals could be recorded before the powder material had begun to settle.

To perform the experiments the model was instrumented in the following way. Three micro-accelerometers were located on its deck, as shown in Fig. 2 and Fig. 3(a): two on the deck edge in a parallel direction to one of the former two, allowing the detection of torsional frequencies and modes besides flexural ones. For the detection of flexural mode shapes, four other micro-accelerometers were conveniently located on one model leg along its height, as shown in Fig. 3(b) and Fig. 4. Detection of flexural modes of the risers was also made possible by locating four micro-accelerometers along their height, as shown in Fig. 3(b). The used micro-accelerometers were of a piezo-resistive water-proof type with a 0 to 2-g range, fabricated by Kyowa Electronic Equipments Company, Japan.

The natural frequencies were determined through spectral analysis of the accelerometer signals recorded from impact tests. The impacts were performed by striking the model at its deck level with the finger tip: centrally in the x and y directions for flexural excitation, and eccentrically for inducing torsion modes. Figure 5 shows

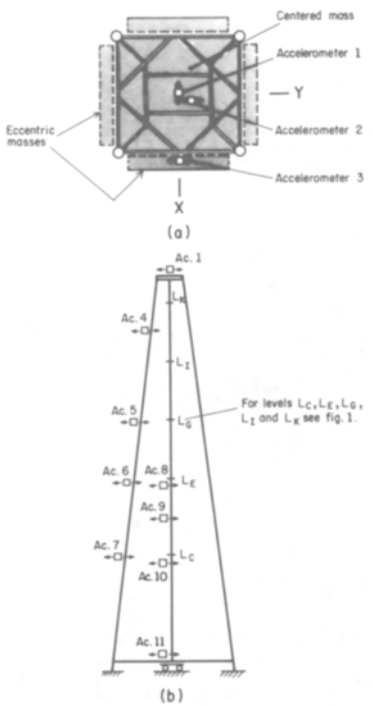

Fig. 3—Model instrumented with accelerometers

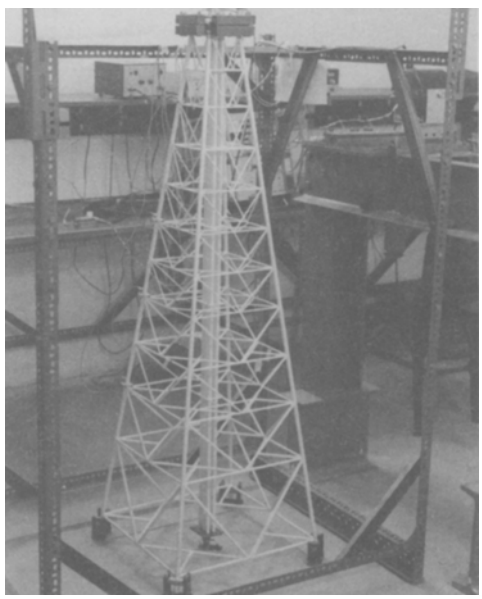

Fig. 4—Instrumentation of one of the legs with accelerometers

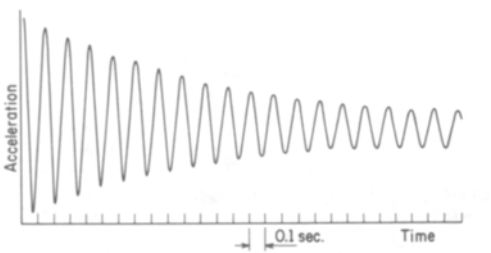

Fig. 5—Response of accelerometer 1 [see Fig. 3(a)] for an impulse in the x direction

one of the recorded acceleration signals. Figure 6 shows the frequency spectrum of acceleration from the time response of the model vibrating in the air.

The mode shapes of vibration, associated with the natural frequencies indicated in Fig. 6, were obtained under forced harmonic excitation of the model in these natural frequencies, i.e., in resonance. A harmonic excitation force of low magnitude was applied in the x and y directions, centrally or eccentrically at the deck level. Some of these mode shapes are depicted in Fig. 7. They were measured by recording simultaneously time response of the five accelerometers located along the height of the model legs or central risers. By normalizing the acceleration amplitudes from each sensor with respect to the maximum acceleration amplitude and observing their phase angles, the mode shapes could then be drawn as depicted in Fig. 7.

Frequency Test Results for the Model in Air

Table 2 presents, for the natural frequencies, f, a comparison between the theoretical results obtained via the FEM model of the prototype vibrating in the air and the experimental results obtained from the hydroelastic reduced model.

As seen in Table 2, the frequency values show, in general, a favorable comparison which demonstrates the reliability of the techniques used in the modeling, construction and experimental measurements and analysis. The major differences found between theoretical and experimental values are referred to the second torsional and third flexural global vibration modes. These differences are due to both the distribution mass along the model height and the axial stiffness of the physical model (see Table 1). It should be emphasized that the latter two influences on the lower modes were counterbalanced by arranging some additional mass on the model deck, as noted in the previous section.

TABLE 2—PROTOTYPE AND REDUCED MODEL NATURAL VIBRATION FREQUENCIES IN AIR (Hz)

	Vibration Modes	Experimental* Extrapolated from Reduced Model	Theoretical FEM Model of Prototype
Global Modes	1st flexural	0.86 ± 0.02	0.86
	1st torsional	2.20 ± 0.04	2.06
	2nd flexural	3.37 ± 0.08	3.23
	2nd torsional	5.62 ± 0.10	4.16
	3rd flexural	6.55 ± 0.20	5.85
Local Modes (Risers)	1st flexural	0.78 ± 0.02	0.82
	2nd flexural	2.27 ± 0.04	2.44
	3rd flexural	4.28 ± 0.08	4.86

*$f_{prot} = \sqrt{k_L}\, f_{model}$; k_L = geometric scale

TABLE 3—NATURAL FREQUENCIES, f, (Hz) FOR THE PROTOTYPE VIBRATING IN STILL WATER AND FOR REDUCED MODEL VIBRATING IN STILL HEAVY FLUID

Global Vibration Modes	Experimental* Extrapolated from Reduced Model	Theoretical FEM Model of Prototype
First Flexural	0.70 ± 0.02	0.79
First Torsional	2.20 ± 0.04	1.97
Second Flexural	2.71 ± 0.08	2.92

$f_{prot} = \sqrt{k_L}\, f_{model}$; k_L = geometric scale

Frequency Test Results for the Model in Fluid

Table 3 presents, for the natural frequencies, f, a comparison between the theoretical results obtained via FEM from the modeled prototype vibrating in water and the experimental results obtained from the hydroelastic reduced model. The latter results were obtained from impact tests in still heavy fluid, transformed according to the frequency scale given by the similitude theory.[3]

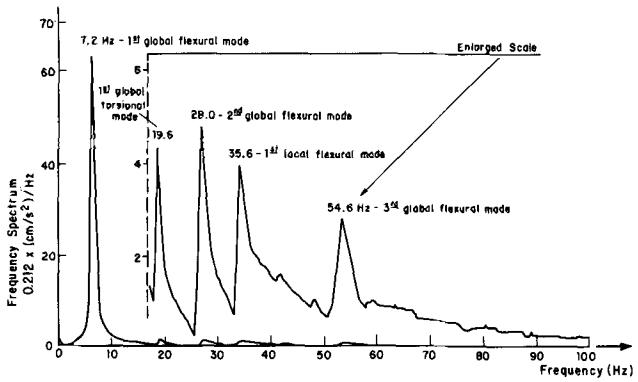

Fig. 6—Frequency spectrum from accelerometer 1 [see Fig. 3(a)]

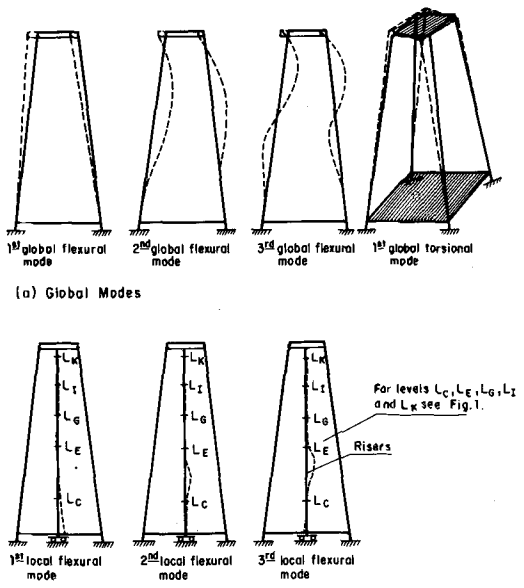

Fig. 7—Vibration modes of the reduced scale model

It should be noted that the value of the inertia coefficient used within the Morison equation for the theoretical FEM model was $C_M = 2.0$, which is the value usually adopted[7-10] in the analysis and design of slender tubular offshore structures displaying a linear behavior. It can be seen from Table 3 that the theoretical frequency values obtained by using $C_M = 2.0$ compare favorably with their experimental counterparts.

Structural Integrity Estimates

With the support conditions fixed and the mass to stiffness ratios adjusted for the structural components, the free vibration response in air of the resulting physical model could not be changed by any factors other than the deck-mass vibrations, which can occur in the prototype counterpart during work conditions.

With this latter fact in mind, an experimental investigation was made of the effects of the variation of deck mass on the natural frequencies and their associated modes. For this, the total amount of deck mass was incremented while its location was approximately maintained. Figure 8 shows clearly these effects by plotting the resulting frequencies ratios (f/f_0) against the total increased mass ratio (m/m_0). In this figure f_0 are some natural frequencies associated with the original mass, m_0.

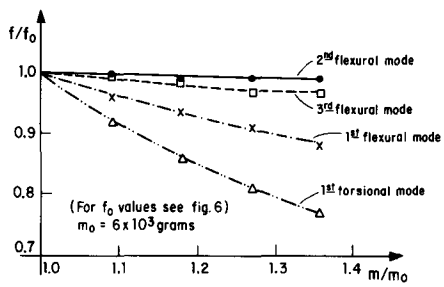

Fig. 8—Influence of deck mass variation on natural frequencies associated with the global modes

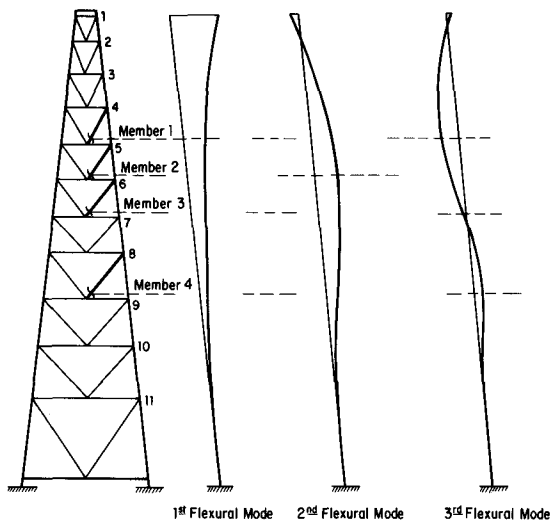

Fig. 9—Location of damaged joints in relation with global natural modes

It can be seen in this figure that, while for the first flexural and first torsional global modes the natural frequencies, f, are reduced with the increasing of mass on the deck, the higher global flexural modes (second and third) are almost insensitive to deck-mass variations. This latter fact was expected as the top model is close to the node point of the second and third vibration modes. The importance of this experimental result seems to be evident: the lack of sensitivity to deck-mass variation of the higher flexural modes indicates that changes in related frequency values could be possible only if the structural integrity is destroyed.

To show the conditions under which the higher flexural modes are most sensitive to local joint damages, vibration tests were carried out on the model which has for each test an isolated cracked joint. The joints indicated in Fig. 9 were partially cracked one at a time for each vibration test. The selection of these joints (on the extremities of diagonal members 1-4, Fig. 9) was made on the basis that mode regions with greater curvatures or changes are those which contain the most stressed members, and that diagonals are more sensitive than horizontal members. Table 4 presents the percent reduction of natural frequency in the model due to damage in the joint. These reductions are, of course, the ratios of values obtained for the damaged and undamaged model.

Some observations can be made from Fig. 9 and Table 4. The first global flexural mode is practically insensitive to joint damages in diagonal members. Other global modes are either sensitive or insensitive to joint damages as measured by changes in their associated natural frequencies, depending on the spatial location of the damaged member. If a damaged member is close to the concavity of a higher flexural mode (second and third modes), the associated natural frequency suffers substantial reduction (mainly for the third global flexural mode). This latter observation seems to be the most relevant as these two modes (second and third flexural) are insensitive to deck-mass variations.

Test Results for Damping

The damping factors associated with the first flexural mode were calculated by the logarithmic decrement technique applied to an acceleration signal (Fig. 5) recorded from impact tests. For the model vibrating in air, the average value found for structural damping, ξ_s, was 0.97 percent.[4] This value lies within the expected range for structural damping of space frame steel structures with fixed supports.[9]

The same procedure for damping calculations was used for the model vibrating in still fluids. Figure 10 shows the variation of total damping factor ($\xi = \xi_s + \xi_f$) with increasing fluid density ϱ_f. It should be emphasized that the additional damping factor, ξ_f, due to the fluid-structure

TABLE 4—REDUCTION IN MODEL NATURAL FREQUENCIES DUE TO DAMAGE IN MEMBER JOINTS

Vibration Modes	Member 1 (percent)	Member 2 (percent)	Member 3 (percent)	Member 4 (percent)
First Flexural	1.7	1.1	0.7	0.3
Second Flexural	2.8	5.0	1.1	0.4
Third Flexural	9.1	3.3	3.6	0.4

interaction is highly dependent on kinematic viscosity. Moreover, the value of viscosity is dependent on the density of the suspension used. In tests, samples of the fluid suspension displayed a non-Newtonian behavior and the experimental data obtained from a viscosimeter was approximated[4] by a plastic model of Bingham. With these calculated values for the kinematic viscosity, ν_f, it was possible to get the corrected damping factors, ξ_f, in the following way.

$$\xi_f = \xi - \xi_s \tag{14}$$

$$\bar{\xi}_f = \frac{\xi_f}{(\nu_f/\nu_{water})^{1/2}} \tag{15}$$

$$\bar{\xi} = \xi_s + \bar{\xi}_f \tag{16}$$

where $\bar{\xi}$ is the total corrected damping factor for the model vibrating in still fluid. It should be noted that correction was made only on the viscous damping, as any other damping contribution originating from the fluid-structure interactive process is negligible[8] within the range of measured displacements. The ratios between displacement amplitudes and diameters of tubular members always stayed under 0.07.

Thus, Fig. 11 shows the variation of the corrected total damping factor, $\bar{\xi}$, with increasing fluid densities, ϱ_f. It can be noted that $\bar{\xi}$ is a 'quasi-linear' function of ϱ_f, and, therefore, extrapolations for higher density fluids can be made. Extrapolation of $\bar{\xi}$ for the ideal model fluid can be seen in Fig. 11, this value being

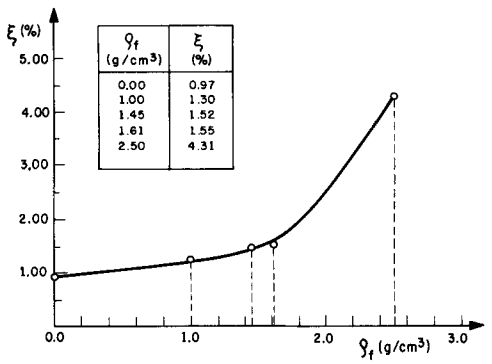

Fig. 10—Variation of total damping factor, ξ, with fluid density, ϱ_f

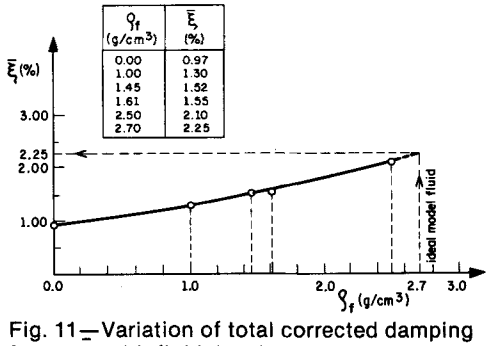

Fig. 11—Variation of total corrected damping factor, $\bar{\xi}$, with fluid density, ϱ_f

$$\bar{\xi} = 2.25 \text{ percent}$$

and, therefore, from eq (16), the value for the fluid damping factor is

$$\bar{\xi}_f = 1.28 \text{ percent}$$

a value which is close to that prescribed by the DNV Rules[9] for prototype of fixed steel towers immersed in water:

$$\xi_f \text{ (DNV)} = 1.5 \text{ percent}$$

In relation to internal damping of the materials used in the model (e.g., ABS polymer, mainly) the authors have yet to obtain any conclusion about its effects on the resulting structural damping. They can only state that the use of the same materials and techniques in other distinct structural models has been successful, as far as the expected damping ratios are concerned.

Concluding Remarks

Study of the hydroelastic reduced model of a fixed offshore structure, designed and fabricated according to the physical conditions imposed by the similitude theory, shows fair agreement between the experimental and theoretical results. Comparing theoretical and experimental results for natural frequencies, it is demonstrated that the techniques used in modeling, construction and experimental analysis are valid and reliable, consequently allowing the extrapolation of the model data to the prototype.

It should be emphasized that the data obtained have a fully experimental character and are undoubtedly relevant for a rational design of this type of offshore structures. But among these data, care should be taken when dealing with the damping factors as they vary from one to another structure, even of the same type. So it is recommended that for design, these damping factors be determined from tests on a similar prototype or, more rationally, from a reduced model fabricated within the similitude conditions.

References

1. Carneiro, F.L.L.B., "Some Aspects of the Dimensional Analysis Applied to the Theory and the Experimentation of Offshore Platforms," Proc. Int. Symp. on Offshore Eng., Pentech Press, London, 542-558 (1982).

2. Roitman, N., Batista, R.C. and Carneiro, F.L.L.B., "Reduced Models for Fixed Offshore Structures," Proc. Int. Symp. on Offshore Eng., Pentech Press, London, 721-740 (1984).

3. Roitman, N., Batista, R.C. and Carneiro, F.L.L.B., "Reduced Model of Fixed Platform for Investigation of Fluid-Structure Interaction," Proc. Int. Symp. on Offshore Eng., Pentech Press, London, 795-804 (1986).

4. Roitman, N., "Hydroelastic Reduced Models for the Dynamic Behavior of Fluid Offshore Platforms," DSc Thesis, in Portuguese, COPPE/UFRJ, Rio de Janeiro (1985).

5. Rosa, S.R., Roitman, N. and Batista, R.C., "Water Depth Influence on the Damping Factors of Jack-up Reduced Models," Proc. Int. Symp. on Offshore Eng., Pentech Press, London, 734-747 (1988).

6. Freire, A.C.G., Roitman, N. and Batista, R.C., "An Experimental Model Study for Deep Water TLP Platform," Proc. Int. Symp. on Offshore Eng., Pentech Press, London, 762-777 (1988).

7. Shore Protection Manual, Publication of U.S. Coast Guard.

8. Sarpkaya, T. and Isaacson, M., Mechanics of Wave Forces on Offshore Structures, Van Nostrand Reinhold Company (1981).

9. Det Norske Veritas - Rules for the Design, Construction and Inspection of Offshore Structures, Oslo, Norway (1977).

10. British Ship Research Association, "A Critical Evaluation of Data on Wave Force Coefficients," Rep. No. 278.12 (Aug. 1976).